Progress In Electromagnetics Research, PIER 70, 307–328, 2007

MODEL COMPUTATIONS OF ANGULAR POWER SPECTRA FOR ANISOTROPIC ABSORPTIVE TURBULENT MAGNETIZED PLASMA

G. V. Jandieri

Physics Department
Georgian Technical University
77 Kostava str. 0175, Tbilisi, Georgia

A. Ishimaru

Department of Electrical Engineering
University of Washington
FT-10 Seattle, Washington 98 195, USA

V. G. Jandieri and A. G. Khantadze

Physics Department
Faculty of Exact and Natural Sciences
Tbilisi State University
3 Chavchavadze str. 0128, Tbilisi, Georgia

Z. M. Diasamidze

Physics Department
Georgian Technical University
77 Kostava str. 0175, Tbilisi, Georgia

Abstract—Electromagnetic waves scattering in turbulent anisotropic collision magnetized ionospheric plasma is investigated using complex geometrical optics approximation. Correlation function of the phase fluctuations of scattered radiation is obtained taking into account both electron density and magnetic fields fluctuations. The features of the angular power spectrum of scattered radiation are investigated analytically and numerically. The expressions of broadening of the spatial spectrum have been obtained for both power-law and anisotropic Gaussian correlation functions of electron density fluctuations. Gaussian spectral function takes into account the axial ratio of the field-aligned irregularities and the angle of inclination of prolate irregularities with respect to the external magnetic field. The variance of the phase and scintillation level of scattered radiation are calculated numerically for F-region irregularities of the ionosphere. The conditions of non-fully and fully developed diffraction patterns have been determined.

1. INTRODUCTION

At the present time the features of light propagation in random media have been rather well studied [1]. Many excellent reviews related to EM waves propagation and observations [2, 3] in the ionosphere have been published, whereas statistical characteristics of scattered radiation are less studied. In most of the papers statistically isotropic irregularities have been considered. However, in reality, irregularities in the ionosphere are anisotropic and mainly elongated along the geomagnetic field. Investigation of statistical characteristics of scattered radiation in randomly inhomogeneous magnetized plasma is of great practical importance. Multiple scattering of EM waves by a plane layer of turbulent collision magnetized plasma has been studied in [4]. The influence of the distance between the emitter and the receiver has been analysed analytically and numerically. Effect of electron density fluctuations on the shape of the angular (spatial) power spectrum (APS) of scattered radiation at arbitrary angles of refraction on plasma vacuum boundary and inclination of the external magnetic field has been investigated in small-angle scattering approximation using the geometrical optics approximation [5, 6]. Statistical simulation has been made utilizing Monte Carlo method. The simulated results have shown that the APS has a double-humped shape, which is caused due to the mutual effects of anisotropy, absorption and shape of the single-scattering phase function. The features of statistical characteristics of the APS of scattered radiation (broadening and shift of its maximum) in turbulent collisionless magnetized plasma have been considered in [7] on the basis of stochastic eikonal equation.

In Section 2 of this paper, general expression of the phase fluctuation is given in complex ray-(optics) approximation. General analytical expressions of statistical characteristics of the APS of scattered radiation are obtained in Section 3. They are expressed through the power spectrum of spatial correlation functions of both electron density irregularities and magnetic field fluctuations. The power-law and anisotropic Gaussian 3D power spectrum are reviewed in Section 4. These results are applied to radio propagation in turbulent collision magnetized plasma as the wavefront travels away from the vacuum-plasma boundary (Section 5). In Section 6, the theory is applied to the F-region of ionosphere; scintillation index has been computed. Conclusion is given in Section 7.

2. FORMULATION OF THE PROBLEM

Let a plane EM wave with frequency ω be incident from vacuum on a semi-infinite slab of turbulent collision magnetized plasma. We choose a Cartesian coordinate system such that XY plane is the vacuum-plasma boundary, Z axis is directed in the plasma slab, YZ plane is generated by the external magnetic field vector $\mathbf{B}_0$ and the wavevector $\mathbf{k}$ of the refracted wave. Electrical features of the ionospheric plasma layer are described by second rank tensor [8]:

$$\tilde{\varepsilon}_{xx}=\tilde{\varepsilon}_{yy} \equiv \tilde{\eta} = 1 = \frac{v(1-is)}{(1-is)^2-u},\ \tilde{\varepsilon}_{xy} = -\tilde{\varepsilon}_{yx} \equiv \tilde{\mu} = -i\frac{v\sqrt{u}}{(1-is)^2-u},$$
$$\tilde{\varepsilon}_{zz} \equiv 1 - \frac{v}{1-is},$$
$$\tilde{\varepsilon}_{xz} = \tilde{\varepsilon}_{zx} = \tilde{\varepsilon}_{yz} = \tilde{\varepsilon}_{zy} = 0, \tag{1}$$

where: $u = \omega_H^2/\omega^2$, $v = \omega_p^2/\omega^2$ and $s = \nu_{eff}/\omega$ are non-dimensional plasma parameters, $\omega_p = (4\pi e^2 N/m)^{1/2}$ is the electron plasma frequency, N is electron density, $\omega_H = |e|H/mc$ is the electron gyrofrequency, $\omega = 2\pi f$, f is frequency of the wave, e and m are the charge and mass of an electron, c is the speed of light in vacuum, N and H are the function of the spatial coordinates, ν_{eff} is the effective electron collision frequency. Frequency of the incident wave is assumed to be much higher than the plasma frequency. The general dispersion relation and analytic expressions for dyadic Green's functions for electrically gyrotropic medium, particularly for ionosphere have been obtained in [9, 10].

Assuming $\tilde{\varepsilon}_{ik}$ to be time independent, electric field $\mathbf{E}$ satisfies the differential equation:

$$\left(\frac{\partial^2}{\partial x_i \partial x_k} - \Delta\delta_{ik} - k_0^2\tilde{\varepsilon}_{ik}\right) E_k = 0, \tag{2}$$

where $\tilde{\varepsilon}_{ik}$ is the relative complex permittivity tensor, which is expressed through the medium parameters determined by (1), $k_0 = \omega/c$ is the wavenumber. We assume that the characteristic spatial scale of inhomogeneities is much greater that the wavelength λ. This assumption enables us to utilize geometrical optics approximation ignoring the interaction between normal waves. Solution of the Equation (2) is sought as $E_i(\mathbf{r}) = A_i(\mathbf{r})\exp[i\tilde{S}(\mathbf{r})]$. Substituting this expression into (2), for the complex phase $\tilde{S}(\mathbf{r})$ we have:

$$Det\left[\left(\Delta\tilde{S}\right)^2\delta_{ik} - \frac{\partial\tilde{S}}{\partial x_i}\frac{\partial\tilde{S}}{\partial x_k} - k_0^2\tilde{\varepsilon}_{ik}\right] = 0. \tag{3}$$

We investigate statistical characteristics of scattered radiation in turbulent magnetized plasma caused by phase fluctuations, as in ray-(optics) approximation phase fluctuations substantially exceed the amplitude fluctuations [1, 11].

Dielectric permittivity submit as sum $\tilde{\varepsilon}_{ik} =< \tilde{\varepsilon}_{ik} > +\delta\tilde{\varepsilon}_{ik}$ ($< \tilde{\varepsilon}_{ik} >\gg \delta\tilde{\varepsilon}_{ik}$, the angular brackets indicate the ensemble average) of the mean and fluctuating components caused due to both electron density (N) and magnetic field (H) fluctuations:

$$\delta\tilde{\varepsilon}_{ik} = \left(\frac{\partial\tilde{\varepsilon}_{ik}}{\partial N}\right)_H N_1 + \left(\frac{\partial\tilde{\varepsilon}_{ik}}{\partial H}\right)_N H_1. \tag{4}$$

As fluctuations of both electron density N_1 and magnetic field H_1 are random functions of spatial coordinates, solution of Equation (3) we will seek as:

$$\tilde{S}(\mathbf{r}) = k_0\tilde{N}(\boldsymbol{\tau}\mathbf{r}) + \tilde{\varphi}_1(\mathbf{r}), \tag{5}$$

where $\tilde{N}$ is complex refractive index of cold collision magnetized plasma [8]:

$$\tilde{N}^2 \equiv (N_* - i\text{æ})^2 = 1 - \frac{2v(1-v-is)}{2(1-is)(1-v-is) - u\sin^2\theta \pm\sqrt{u^2\sin^4\theta + 4u(1-v-is)\cos^2\theta}} \tag{6}$$

Signs "+" and "−" refer to the ordinary and extraordinary waves, respectively; æ is an absorption coefficient, θ is the angle between the direction of wave propagation $\mathbf{k}$ and the geomagnetic field $\mathbf{B}_0$, $\boldsymbol{\tau}$ is the unit vector along wave propagation, $\tilde{\varphi}_1$ is phase fluctuation of scattered wave. Without loss of generality we assume that the vector $\boldsymbol{\tau}$ lies in YZ plane (principle plane).

Substituting (5) into (3), in a zero approximation complex refractive index satisfies the equation $(\nabla\tilde{S})^2 = k_0^2\tilde{N}^2$. Fluctuation component of the complex phase satisfies linear stochastic differential equation:

$$a_y\frac{\partial\tilde{\varphi}}{\partial y} + a_z\frac{\partial\tilde{\varphi}_1}{\partial z} = k_0\left(k_0 A_\nu\delta\nu + A_h\delta h\right), \tag{7}$$

with

$$
\begin{aligned}
a &= \left(a'_z a''_y - a'_y a''_z\right)/a'^2_z,\ b = a'_y/a'_z,\\
a_y &= a'_y + i a''_y,\\
a'_y &= N_* \sin\theta \left[\left(\eta' - n_1^2\right)\left(\eta' + \varepsilon'\right) + \sin^2\theta \cdot n_1^2\left(\varepsilon' - \eta'\right) - \mu''^2\right],\\
a''_y &= N_* \sin\theta \left\{\left(\eta' + \varepsilon'\right)\left(n_2^2 - \eta''\right) - \left(\eta' - n_1^2\right)\left(\eta'' + \varepsilon''\right)\right.\\
&\quad \left. + \sin^2\theta\left[n_1^2\left(\eta'' - \varepsilon''\right) - n_2^2\left(\varepsilon' - \eta'\right)\right] - 2\mu'\mu''\right\},\\
a_z &= a'_z + i a''_z,\\
a'_z &= N_* \cos\theta\left[2\varepsilon'\left(\eta' - n_1^2\right) + \sin^2\theta \cdot n_1^2\left(\varepsilon' - \eta'\right)\right],\\
a''_z &= N_* \cos\theta\left\{2\left[\varepsilon'\left(n_2^2 - \eta''\right) - \varepsilon''\left(\eta' - n_1^2\right)\right]\right.\\
&\quad \left. + \sin^2\theta\left[n_1^2\left(\eta'' - \varepsilon''\right) - n_2^2\left(\varepsilon' - \eta'\right)\right]\right\},\\
A_\nu &= A'_\nu + A''_\nu,\\
A'_\nu &= \varepsilon'\left(\eta' - n_1^2\right)\left(\eta' - 1\right) + \frac{1}{2}\sin^2\theta n_1^2\left(\eta' - 1\right)\left(n_1^2 - 2\eta' + \varepsilon'\right)\\
&\quad + \frac{1}{2}\left(n_1^2 - \eta'\right)\left(n_1^2\cos^2\theta - \eta'\right)\left(\varepsilon' - 1\right)\\
&\quad - \frac{1}{2}\mu''^2\left(\varepsilon' - 1\right) - \mu''^2\left(\varepsilon' - n_1^2\sin^2\theta\right),\\
A''_\nu &= \left[\varepsilon'\left(n_2^2 - \eta''\right) - \varepsilon''\left(\eta' - n_1^2\right)\right]\left(\eta' - 1\right) - \varepsilon'\left(\eta' - n_1^2\right)\eta''\\
&\quad - \frac{1}{2}\sin^2\theta\left\{n_1^2\left(\eta' - 1\right)\left(n_2^2 - 2\eta'' + \varepsilon''\right)\right.\\
&\quad \left. + \left[n_2^2(\eta' - 1) + n_1^2\eta''\right]\left(n_1^2 - 2\eta' + \varepsilon'\right)\right\} - \frac{1}{2}\left(n_1^2 - \eta'\right)\left(n_1^2\cos^2\theta - \eta'\right)\varepsilon''\\
&\quad + \frac{1}{2}(\varepsilon' - 1)\left[\left(n_1^2 - \eta'\right)\left(\eta'' - n_2^2\cos^2\theta\right) + \left(\eta'' - n_2^2\right)\left(n_1^2\cos^2\theta - \eta'\right)\right]\\
&\quad - \frac{1}{2}\left[-\varepsilon''\mu''^2 + 2\mu'\mu''\left(\varepsilon' - 1\right)\right] - \mu''^2\left(n_2^2\sin^2\theta - \varepsilon''\right)\\
&\quad - 2\mu'\mu''\left(\varepsilon' - n_1^2\sin\theta\right)\\
A_h &= A'_h + A''_h,\\
A'_h &= \frac{1}{1-u}\left\{\left(\eta' - n_1^2\right)\varepsilon'(\eta' - 1)u + \frac{1}{2}u\sin^2\theta n_1^2(\eta' - 1)\left(n_1^2 - 2\eta' + \varepsilon'\right)\right.\\
&\quad \left. + \mu'^2\left(\varepsilon' - n_1^2\sin^2\theta\right)\right\},
\end{aligned}
$$

$$\begin{aligned}
A_h'' &= \frac{u}{1-u}\left\{\left(n_2^2-\eta''\right)\varepsilon'\left(\eta'-1\right)-\left(\eta'-n_1^2\right)\left[\varepsilon''\left(\eta'-1\right)+\eta''\varepsilon'\right]\right\}\\
&\quad+\frac{u\sin^2\theta}{2(1-u)}\left\{n_1^2\left(\eta'-1\right)\left(2\eta''-n_2^2-\varepsilon''\right)\right.\\
&\quad\left.-\left[n_1^2\eta''+n_2^2\left(\eta'-1\right)\right]\left(n_1^2-2\eta'+\varepsilon'\right)\right\}\\
&\quad+\frac{1}{1-u}\left[\mu'^2\left(n_2^2\sin^2\theta-\varepsilon''\right)-2\mu'\mu''\left(\varepsilon'-n_1^2\sin^2\theta\right)\right], \qquad (8)
\end{aligned}$$

where real and imaginary components in (8) are determined as [8]:

$$\tilde{\eta}=\eta'-i\eta''=1=\frac{v\left(1+s^2-u\right)}{\left(1-s^2-u\right)^2+4s^2}-i\frac{sv\left(1+s^2+u\right)}{\left(1-s^2-u\right)^2+4s^2},$$

$$\tilde{\mu}=\mu'-i\mu''=\frac{2sv\sqrt{u}}{\left(1+s^2-u\right)^2+4s^2}-i\frac{v\sqrt{u}\left(1-s^2-u\right)}{\left(1+s^2-u\right)^2+4s^2},$$

$$\tilde{\varepsilon}=\varepsilon'-i\varepsilon''=1-\frac{v}{1+s^2}-i\frac{sv}{1+s^2}.$$

$n_1^2=N_*^2-æ^2$ and $n_2^2=2N_*æ$,

$$N_*^2-æ^2=1-2v\frac{(1-v)\left[2(1-v-s^2)-u\sin^2\theta\pm P\right]-s[2s(v-2)\pm U]}{\left[2\left(1-v-s^2\right)-u\sin^2\theta\pm P\right]^2+[2s(v-2)\pm U]^2},$$

$$N_*æ=-v\frac{s\left[2(1-v-s^2)-u\sin^2\theta\pm P\right]+(1-v)[2s(v-2)\pm U]}{\left[2\left(1-v-s^2\right)-u\sin^2\theta\pm P\right]^2+[2s(v-2)\pm U]^2},$$

$$P+iU\equiv\sqrt{p+iq}=\sqrt{0,5\left(\sqrt{p^2+q^2}+p\right)}+i\sqrt{0,5\left(\sqrt{p^2+q^2}-p\right)},$$

$$q=8su(v-1)\cos^2\theta,\ p=u^2\sin^4\theta+4u\left[(v-1)^2-s^2\right]\cos^2\theta.$$

Fluctuation component of the phase expand in terms of 2-D Fourier transform:

$$\tilde{\varphi}_1(x,y,z)=\int_{\infty}^{\infty}dk_x\int_{\infty}^{\infty}dk_y\tilde{\varphi}_1\left(k_x,k_y,z\right)\exp\left(ik_xx+ik_yy\right), \qquad (9)$$

with the boundary condition $\tilde{\varphi}_1|_{z=0}$. As a result the solution of Equation (7) can be written as

$$\tilde{\varphi}_1(x,y,z)\ =\ k_0\int_{\infty}^{\infty}dk_x\int_{\infty}^{\infty}dk_y\exp\left(ik_xx+ik_yy\right)$$

$$\left\{\left[\frac{D}{N_0}\int_0^z d\xi N_1\left(k_x,k_y,\xi\right)+\frac{F}{H_0}\int_0^z d\xi H_1\left(k_x,k_y,\xi\right)\right]\right.$$
$$\left.+i\left[\frac{E}{N_0}\int_0^z d\xi N_1\left(k_x,k_y,\xi\right)+\frac{G}{H_0}\int_0^z d\xi H_1\left(k_x,k_y,\xi\right)\right]\right\}$$
$$\exp[(-a+ib)k_y(\xi-z)], \tag{10}$$

the distance z traveling by the wave in turbulent collision magnetized plasma satisfies the condition $z \ll k_0\ell_i^2$ ($\ell_i = \min\{\ell_N, \ell_H\}$), ℓ_N and ℓ_H are characteristic spatial scales of electron density and magnetic field fluctuations), $D = A'_\nu/a'_z$, $E = \left(A''_\nu a'_z - A'_\nu a''_z\right)/a'^2_z$, $F = A'_h/a'_z$, $G = \left(A''_h a'_z - A'_h a''_z\right)/a'^2_z$.

3. STATISTICAL CHARACTERISTICS OF THE ANGULAR POWER SPECTRUM

Relationship between the transverse correlation function of the phase fluctuations, caused due to large-scale irregularities ($\lambda/2\pi\ell \ll 1$, λ is the radio wavelength) and the 3-D spectral shapes of both electron density $W_N\left(k_x,k_y,k_z\right)$ and magnetic field fluctuations $W_H\left(k_x,k_y,k_z\right)$, having in general different characteristic spatial scales (we took into account statistical independence of $\delta\nu = N_1/N_0$ and $\delta h = H_1/H_0$), for turbulent collision magnetized plasma is expressed as follows:

$$\begin{aligned} W_\varphi\left(\rho_x,\rho_y,z\right) &= <\tilde{\varphi}_1\left(x+\rho_x,y+\rho_y,z\right)\tilde{\varphi}_1^*(x,y,z)>=2\pi k_0^2 \\ &\int_{-\infty}^{\infty} d\kappa_x \int_{-\infty}^{\infty} d\kappa_y \left[\left(D^2+E^2\right)\sigma_N^2 W_N\left(\kappa_x,\kappa_y,-b\kappa_y\right)\right. \\ &\left.+\left(F^2+G^2\right)\sigma_H^2 W_H\left(\kappa_x,\kappa_y,-b\kappa_y\right)\right]\frac{1}{2a\kappa_y} \\ &[1-\exp(-2a\kappa_y z)]\exp(i\kappa_x\rho_x+i\kappa_y\rho_y+2a\kappa_y z). \end{aligned} \tag{11}$$

Here $\sigma_N^2 \equiv <N_1^2>/N_0^2$ and $\sigma_H^2 \equiv <H_1^2>/H_0^2$ are variances of electron density and magnetic field fluctuations, respectively; k_x and k_y are components of wavevector perpendicular to the magnetic field. Equation (11) takes into account the oblique refraction of the wave with respect to the imposed external magnetic field, anisotropy of irregularities, dip angle of elongation of stretched inhomogeneities with respect to the propagation of electromagnetic wave and fluctuations of magnetic field. For turbulent collisionless magnetized plasma $s = 0$, assuming that $\theta = 0°$ coefficients in Equation (11) are equal to: $a = 0$,

$E = 0$, $D^2 = v^2/(1 \pm \sqrt{u})^2 [1 - v/1 \pm \sqrt{u}]$. In high frequency bands, $u \ll 1$, $D^2 k_0^2 = N_0^2 (r_e \lambda)^2$ (r_e is the classical electron radius) we obtain the well-known formula [12]: $W_\varphi (k_x, k_y, z) = 2\pi < N_1^2 > (r_e \lambda)^2 z W_N (k_x, k_y, 0)$.

Correlation function of the complex field could be written as [4–7]:

$$\begin{aligned} W_E (\rho_x, \rho_y, z) &= < E (x + \rho_x, y + \rho_y, z) E^*(x, y, z) > \\ &= E_0^2 \exp [i k_y \rho_y - 2 (\mathrm{Im} k_z) z] \times \\ &\quad \times < \exp\{i\varphi_1(x+\rho_x, y+\rho_y, z) - i\varphi_1^*(x, y, z)\} >. \end{aligned} \quad (12)$$

It should be mentioned that the imaginary part of the wavenumber $k_z = \sqrt{\left(\omega^2 \tilde{N}^2/c^2\right) - k_y^2}$ appears in (12) as the argument of the exponential term and its contribution to the statistical parameters of phase fluctuations increases in proportion to the distance z. In the most interesting case of multiple scattering, when the phase fluctuations are strong $< \varphi_1 \varphi_1^* > \gg 1$, we can assume that they are normally distributed [1, 11].

Correlation function sharply decreases as ρ_x and ρ_y increase and the argument of the second exponential term could be expanded into a series as follows [4–7]:

$$\begin{aligned} W_E (\rho_x, \rho_y, z) &= E_0^2 \exp [i k_y \rho_y - 2 (\mathrm{Im} k_z) z] \\ &\quad \exp \left(\frac{\partial W_\varphi}{\partial \rho_y} \rho_y + \frac{1}{2} \frac{\partial^2 W_\varphi}{\partial \rho_x^2} \rho_x^2 + \frac{1}{2} \frac{\partial^2 W_\varphi}{\partial \rho_y^2} \rho_y^2 \right), \end{aligned} \quad (13)$$

where the phase correlation function W_φ is given by (11). The derivatives of the phase correlation function are taken at $\rho_x = \rho_y = 0$.

The 2-D APS of scattered radiation could be defined in terms of Fourier transformation of the 3-D spatial correlation function [11]:

$$S (k_x, k_y, z) = \frac{1}{(2\pi)^2} \int_{\infty}^{\infty} d\rho_x d\rho_y W_E (\rho_x, \rho_y, z) \exp (-i k_x \rho_x - i k_y \rho_y). \quad (14)$$

This characteristic is equivalent to the ray intensity (brightness) in radiation transport equation [1, 11]. In the most interesting case of strong fluctuation of the phase $< \varphi_1 \varphi_1^* > \gg 1$, APS is expressed as follows [4–7]:

$$S (k_x, k_y, z) = S_0 \exp \left[-\frac{k_x^2}{2 < k_x^2 >} - \frac{(k_y - \Delta k_y)^2}{2 < k_y^2 >} \right], \quad (15)$$

where: S_0 is the amplitude of spectral curve, Δk_y determines the shift of spectral maximum, $< k_y^2 >$ and $< k_x^2 >$ are the broadening of the APS in the principle YZ plane and perpendicular XZ planes, respectively. Knowledge of the phase correlation function allows us to calculate the width of the angular spectrum and the displacement of its maximum utilizing the following expressions [4–7]:

$$\Delta k_y = \frac{1}{i}\frac{\partial W_\varphi}{\partial \rho_y}\bigg|_{\rho_x=\rho_y=0},$$

$$< k_y^2 >= -\frac{\partial^2 W_\varphi}{\partial \rho_y^2}\bigg|_{\rho_x=\rho_y=0}, \quad < k_x^2 >= -\frac{\partial^2 W_\varphi}{\partial \rho_x^2}\bigg|_{\rho_x=\rho_y=0}. \tag{16}$$

The parameter range in which expressions (15) and (16) correctly describe the angular power spectrum of scattered radiation is determined by the following inequalities [5]: $|\Delta k_x| \ll 2\pi/\lambda$, $\sqrt{< k_x^2 >} \ll 2\pi/\lambda$, $\sqrt{< k_y^2 >} \ll 2\pi/\lambda$. These conditions are not in contravention to the assumption of strong phase fluctuations because in a smoothly inhomogeneous medium mean spatial scale of plasma inhomogeneities of the phase correlation function substantially exceeds the wavelength of scattered electromagnetic waves, $\ell \gg \lambda$ [11] and the angle of the normal to the random wavefront $\Delta\theta \propto \lambda\sqrt{< \varphi_1^2 >}/\ell$ can remain small even at $< \varphi_1^2 >\gg 1$. Further we will consider only electron density fluctuations, as we do not have any information about magnetic field fluctuations in F-region of the ionosphere.

4. ANISOTROPIC GAUSSIAN AND POWER-LAW CORRELATION FUNCTIONS

Irregularities that are responsible for fluctuations of radiation from discrete sources and satellites are mainly located in F-region of the ionosphere at a height of $250 \div 400$ km. Data obtained from spaced receiver measurements made at Kingston, Jamaica (during the periods August 1967–January 1969 and June 1970–September 1970) show that the irregularities between heights of 153 and 617 km causing the scintillation of signals from the moving earth satellites (BE-B and BE-C) are closely aligned along the magnetic field lines in the F-region [13]. The orientation of the irregularities in the ionosphere has been measured with respect to the geographic north observing a diffraction pattern of the satellite signals (41 MHz) on the ground. The dip angle of the irregularities with respect to the field lines was within 16°. The anisotropic spectral features in F-region are defined for Gaussian and power-law spectra.

Firstly, we consider the anisotropic Gaussian correlation function describing anisomeric irregularities. Let longitudinal spatial scale of large-scale irregularities $\ell_\parallel$ substantially exceeds a transversal scale $\ell_\perp = \{\ell_x, \ell_y\}$. Generally, the direction of elongated irregularities does not coincide neither with the direction of wave propagation $\boldsymbol{\tau} \in YZ$ (vector $\boldsymbol{\tau}$ makes the angle θ with geomagnetic field), nor with the direction of an external homogeneous magnetic field (along Z axis). If axis X and X' coincide and axis Y' and Z' are rotated at an angle α with respect to the axis Y and Z (α is the orientation angle of anisotropy elongation of irregularities with respect to the external magnetic field), utilizing the rotational matrix the anisotropic 3D Gaussian spatial power spectrum is defined as:

$$W_N(k_x, k_y, k_z) = \sigma_N^2 \frac{\ell_\perp^2 \ell_\parallel}{8\pi^{3/2}} \exp\left\{ -\frac{k_y^2 \ell_\parallel^2}{4} \frac{1}{\chi^2 \cos^2\alpha + \sin^2\alpha} \left[1 + \frac{(1+\chi^2)^2}{\chi^2} \sin^2\alpha \cos^2\alpha \right] - \frac{k_x^2 \ell_\perp^2}{4} - \frac{\chi^2 \cos^2\alpha + \sin^2\alpha}{4\chi^2} k_z^2 \ell_\parallel^2 - \frac{\chi^2 - 1}{2\chi^2} \sin\alpha \cos\alpha \ell_\parallel^2 k_y k_z \right\}. \quad (17)$$

$\chi = \ell_\parallel / \ell_\perp$ is the axial ratio of the field-aligned irregularities defined as a ratio of longitudinal and transversal linear scales of electron density irregularities, k_z is the wavevector component parallel to the geomagnetic field. Expression (17) could be rewritten as:

$$W_N(k_x, k_y, -bk_y) = \sigma_N^2 \frac{\ell_\parallel \ell_\perp^2}{8\pi^{3/2}} \exp\left[-\frac{k_x^2 \ell_\perp^2}{4} - Q^2(\alpha, \chi) \frac{k_y^2 \ell_\parallel^2}{4} \right]. \quad (18)$$

where

$$Q^2(\alpha, \chi) = \frac{1}{\sin^2\alpha + \chi^2 \cos^2\alpha} \left[1 + \frac{(1-\chi^2)^2}{\chi^2} \sin^2\alpha \cos^2\alpha \right] + b^2 \frac{\sin^2\alpha + \chi^2 \cos^2\alpha}{\chi^2} - 2b \frac{\chi^2 - 1}{\chi^2} \sin\alpha \cos\alpha,$$

If we suppose that $k_x = 0$ and $k_y \to k_\perp$, we obtain pictorial illustration of a contour of equal spectral density, isospectroid, for different values of angle of inclination α of prolate irregularities with respect to the external homogeneous magnetic field:

$$m^2 M k_\perp^2 + \frac{\chi^2}{m^2} k_z^2 + 2\left(1 - \chi^2\right)^2 \sin\alpha \cos\alpha k_\perp k_z = const, \quad (19)$$

where $m^2 = \frac{\chi}{\sin^2\alpha + \chi^2\cos^2\alpha}$, $M = 1 + \frac{(1-\chi^2)^2}{\chi^2}\sin^2\alpha\cos^2\alpha$.

For isotropic irregularities $\chi = 1$, isospectroid represents the circle ($k_\perp^2 + k_z^2 = const$) in the principle YOZ plane. Isospectroid for anisotropic Gaussian irregularities is stretched in a plane normal to the magnetic field as presented in Figure 1.

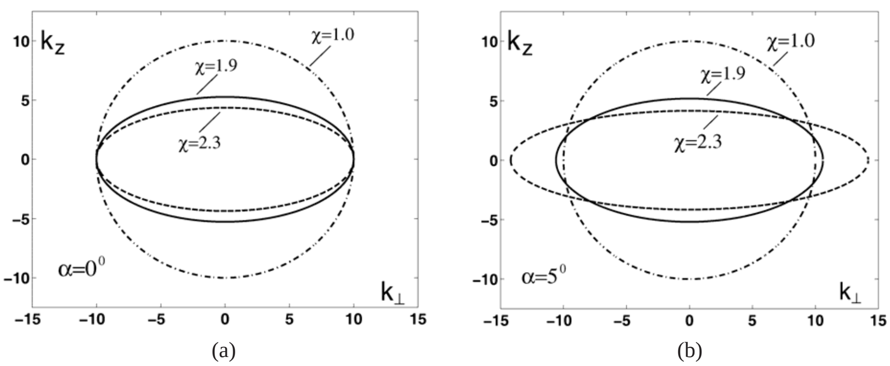

Figure 1. (a) 2D isospectroid for different parameter of anisotropy if prolate irregularities are oriented along the geomagnetic field $\alpha = 0°$, (b) 2D isospectroid for different parameter of anisotropy if the angle of inclination of prolate irregularities with respect to the external magnetic field is $\alpha = 5°$.

Measurements of satellite's signal parameters passing through ionospheric layer and measurements aboard of satellite show that in F-region of the ionosphere irregularities have power-law spectrum with different spatial scales. Observations suggest that the power-law spectrum is believed to be the most suitable model of ionospheric irregularities. We will utilize a model of 3-D anisotropic power-low spectrum of irregularities. Generalized correlation function for power-law spectrum of electron density irregularities with a powerlaw index p has been proposed in [14]. The corresponding spectral function has the form:

$$W_N(\mathbf{k}) = \frac{\sigma_N^2}{(2\pi)^{3/2}} \frac{r_0^3\,(k_0 r_0)^{(p-3)/2}}{\left(r_0\sqrt{k^2+k_0^2}\right)^{p/2}} \frac{K_{p/2}\left(r_0\sqrt{k^2+k_0^2}\right)}{K_{(p-3)/2}\,(k_0 r_0)}, \tag{20}$$

where $K_\nu(x)$ is McDonald function, r_0 is the inner scale of turbulence, $L_0 = 2\pi/k_0$ is the outer scale; it is supposed that $k_0 r_0 \ll 1$. In the interval of wavenumber $k_0 r_0 \ll k r_0 \ll 1$ spatial spectrum is written as [14]:

$$W_N(\mathbf{k}) = \frac{\sigma_N^2}{2\pi} \frac{\Gamma\left(\frac{p}{2}\right)}{\Gamma\left(\frac{3}{2}\right)\Gamma\left(\frac{p-3}{2}\right)} \frac{L_0^3}{\left(1 + L_0^2 k^2\right)^{p/2}}, \tag{21}$$

Utilizing functional expression for the gamma function Γ [15] $\Gamma(z)\Gamma(1-z) = \pi/\sin(\pi z)$, instead of L_0 we introduce two spatial correlation lengths of electron density irregularities $\ell_\parallel$ and $\ell_\perp$. Hence, for $p > 3$ spatial power-law spectrum could be rewritten as:

$$W_N(\mathbf{k}) = \frac{\sigma_N^2}{2\pi^2} \frac{\Gamma\left(\dfrac{p}{2}\right)\Gamma\left(\dfrac{5-p}{2}\right)}{\Gamma\left(\dfrac{3}{2}\right)} \sin\left[\frac{(p-3)\pi}{2}\right] \frac{\ell_\perp^2 \ell_\parallel}{\left[1+\ell_\perp^2\left(k_\perp^2+\chi^2 k_\parallel^2\right)\right]^{p/2}}, \tag{22}$$

Experimental investigations of Doppler frequency shift of ionospheric signal show that index of the power-law spectrum of electron density fluctuations is in the range of $3.8 \leq p \leq 4.6$. Experimental value of the power-law spectrum of the ionosphere ($< p > \approx 4$) , measured by translucence of satellite signals [16], is within the limits of p. Experimental observations of backscattering signals from the artificially disturbed region of the ionosphere by the powerful HF radio emission shows that a lot of artificial ionospheric irregularities of the electron density are stretched along the geomagnetic field. Power-law spectral index was within the limits $p = 1.4 \div 4.8$ for different heating sessions using "Sura" heating facility in the frequency range of $4.7 \div 9$ MHz (ordinary mode) with the effective radiated power $50 \div 70$ MW beamed vertically upwards [17].

5. NUMERICAL CALCULATION OF STATISTICAL CHARACTERISTICS

Knowledge of the correlation function of the phase allows us to calculate both the broadening and displacement of the maximum of the APS in the geometrical optics approximation. Substituting (18) into (16) expression for the broadening of the APS in the principle plane for anisotropic Gaussian power spectrum is obtained:

$$\frac{< k_y^2 >}{k_0^2} = 2\sqrt{\pi}\sigma_N^2\left(D^2 + E^2\right)\frac{z}{Q^3 \ell_\parallel \chi}. \tag{23}$$

Figure 2 illustrates the behavior of the normalized broadening of the APS versus angle of refraction θ. Statistical characteristics are normalized on the wavenumber of an incident EM wave. Numerical calculations for the anisotropic Gaussian power spectrum have been carried out in F-region at a height of 280 km for the basic frequency 40 MHz under the following plasma parameters: $\sigma_N^2 = 10^{-6}$, $k_0\ell_\parallel = 5 \cdot 10^3$, $z/\ell_\parallel = 100$. Figures show that when the angle α between elongated electron density irregularities and external magnetic field increases, amplitude of broadening of the APS decreases. Spatial spectrum narrows in proportion to the parameter of anisotropy χ at a fixed angle α (Figure 2(b)). Simple relationship between a displacement of a maximum of the APS and its broadening could be written as $\Delta k_y = az < k_y^2 >$. Numerical estimations for displacement of maximum of the APS have been made for the fixed angles: $\theta = 20°$ and $\alpha = 5°$: $\Delta k_y/k_0 = 2 \cdot 10^{-7}$ (at $\chi = 3$), $\Delta k_y/k_0 = 5 \cdot 10^{-7}$ (at $\chi = 5$) and $\Delta k_y/k_0 = 6 \cdot 10^{-7}$ (at $\chi = 10$).

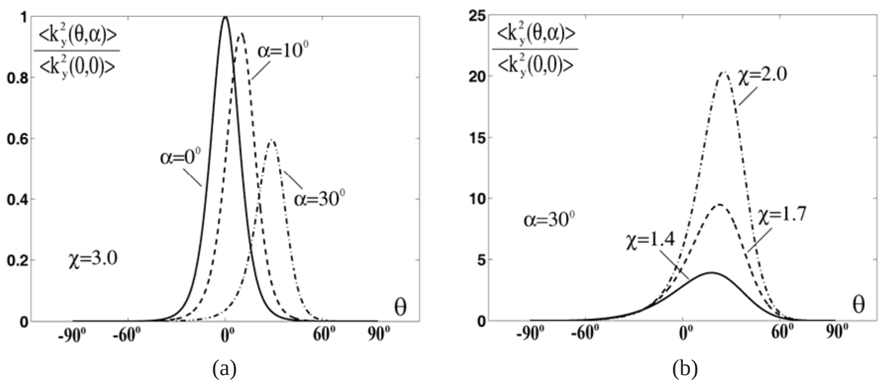

Figure 2. (a) Normalized broadening of the angular power spectrum versus angle of refraction θ for different angle of inclination of prolate irregularities α, parameter of anisotropy $\chi = 3$, (b) normalized broadening of the angular power spectrum versus angle of refraction θ for different parameter of anisotropy χ at angle of inclination of prolate irregularities $\alpha = 30°$.

The phase scintillations are often not measured directly, but rather as a difference of scintillations at two points separated by a distance ρ_y. For simplicity we will consider two observation points in mutually perpendicular directions normal to the radio path. Setting (22) into (11), taking into account smallness of the parameter a and expanding the exponential term into the series, correlation function of the phase has the form:

$$W_\varphi(0,\rho_y,z) = 2^{(4-p)/2}\sigma_N^2\left(D^2+E^2\right)\frac{\Gamma\left(\frac{5-p}{2}\right)}{\Gamma\left(\frac{3}{2}\right)} \sin\left[\frac{(p-3)\pi}{2}\right]\frac{k_0^2 z\ell_\parallel\chi^{(p-2)/2}}{(1+b^2\chi^2)^{p/4}}\left(\frac{\rho_y}{\ell_\parallel}\right)^{(p-2)/2} \times K_{(p-2)/2}\left(\frac{\chi\rho_y}{\ell_\parallel\sqrt{1+b^2\chi^2}}\right). \quad (24)$$

Variance of correlation function of the phase at $p > 3$ is given by the following expression:

$$\sigma_\varphi^2 = \frac{1}{\sqrt{\pi}}\sigma_N^2\left(D^2+E^2\right)\Gamma\left(\frac{5-p}{2}\right)\Gamma\left(\frac{p-2}{2}\right)\sin\left[\frac{(p-3)\pi}{2}\right]\frac{k_0^2 z\ell_\parallel}{\sqrt{1+b^2\chi^2}}. \quad (25)$$

Knowledge of the correlation function of the phase (11) allows us to calculate the broadening of the APS of scattered EM waves caused due to electron density irregularities in turbulent collision magnetized plasma. Utilizing the expression $< k_x^2 > = -\left[\partial^2 W_\varphi(\rho_x,\rho_y,z)/\partial\rho_x^2\right]_{\rho_x=\rho_y=0}$ [5–7] we will have:

$$\frac{<k_x^2>}{k_0^2} = <\sigma_N^2>\left(D^2+E^2\right)\frac{\Gamma\left(\frac{p}{2}\right)\Gamma\left(\frac{5-p}{2}\right)\Gamma\left(\frac{p-4}{2}\right)}{\Gamma\left(\frac{3}{2}\right)\Gamma\left(\frac{p-3}{2}\right)} \times\left[\frac{\Gamma\left(\frac{p-3}{2}\right)}{\Gamma\left(\frac{p-2}{2}\right)}-\frac{\Gamma\left(\frac{p-1}{2}\right)}{\Gamma\left(\frac{p}{2}\right)}\right]\sin\left[\frac{(p-3)\pi}{2}\right]\frac{z\chi^2}{\ell_\parallel(1+b^2\chi^2)^{3/2}}. \quad (26)$$

Broadening of the APS in the principal plane is equal to $\left(< k_y^2 > / k_0^2\right) = \left(< k_x^2 > / k_0^2\right)/\left(1+b^2\chi^2\right)$. Hence, spatial spectrum of scattered radiation in the principal plane narrows inversely proportional to the anisotropy factor χ.

Numerical calculations for the power-law spectrum in F-region of the ionosphere at a height 280 km have been carried out for the following parameters: $k_0\ell_\parallel = 10^4$, $\sigma_N^2 = 10^{-4}$ [18] $z/\ell_\parallel = 7.0$. Figure 3(a) illustrates that normalized correlation function of the phase (NCF) of electron density irregularities decreases in proportion

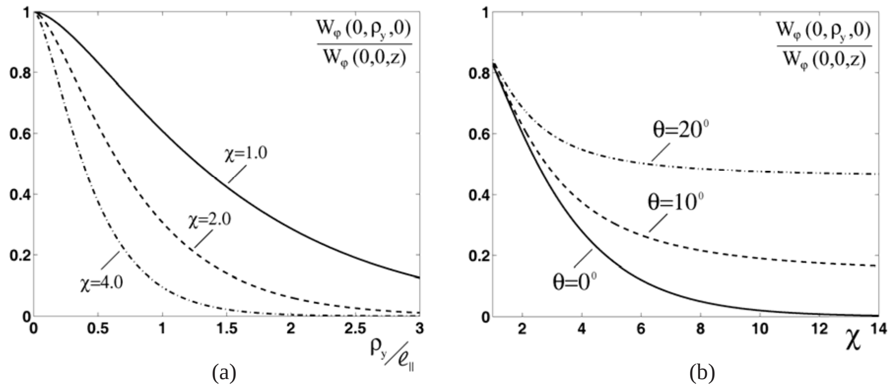

Figure 3. (a) Dependence of the normalized correlation function of the phase of scattered radiation versus normalized distance of the base for different values of anisotropic factor χ, (b) Dependence of the normalized correlation function of the phase of scattered radiation versus anisotropic factor for different values of refraction angle θ ($\rho_y/\ell_\parallel = 0.5$).

to a distance ρ_y normalized on the longitudinal characteristic spatial scale of elongated irregularities $\ell_\parallel$ at $\theta = 10°$ with a power-law index of $p = 4$. Calculations show that curve smoothly decreases in isotropic case ($\chi = 1$). At small distance of $\rho_y/\ell_\parallel$ the curves of NCF sharply decrease inversely proportional to the factor of anisotropy χ. Figure 3(b) illustrates the dependence of the NCF versus parameter of anisotropy χ. With increasing the angle of refraction θ with respect to the external magnetic field, NCF decreases and beginning from $\chi = 13$ tends to saturation (for $\theta = 10°$). Anisotropy of electron density irregularities has a substantially effect on the broadening of the APS of scattered EM waves. Figures 4(a) and 4(b) illustrates the broadening of the spatial spectrum versus coefficient of anisotropy at different angles of refraction $\theta = 10°, 15°, 20°$. Firstly, APS of scattered radiation increases and then smoothly decreases in proportion to the anisotropy factor at a power-law index $p = 4.5$. The reason is that in geometrical optics approximation, in non-absorbing media (neglecting fluctuations) when both amplitude and phase S are real quantities, vector of energy-flux density and vector ∇S are collinear and directed to the normal of the phase front, while in absorptive media the directions of wave propagation ∇S_1 and the direction of fastest dumping of the wave ∇S_2 are not coincided [5, 7]. Particularly, normalized broadening reaches its maximum in XOZ plane at $\chi = 8$ (if $\theta = 10°$); at $\chi = 5.3$ (if $\theta = 15°$)

and at $\chi = 4$ (if $\theta = 20°$); in the principle plane YOZ at $\chi = 4.7$ (if $\theta = 10°$), at $\chi = 3$ (if $\theta = 15°$) and at $\chi = 2.2$ (if $\theta = 20°$).

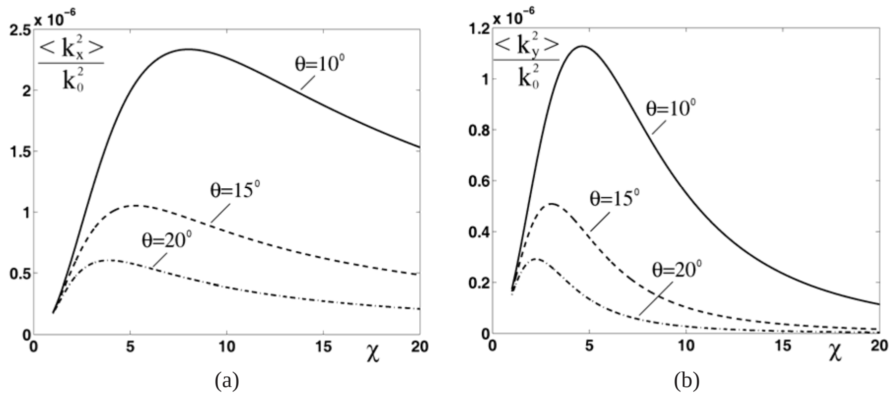

Figure 4. (a) Dependence of the normalized broadening of the angular spectrum versus anisotropic factor for different values of refraction angle θ in XOZ plane, (b) Dependence of the normalized broadening of the angular spectrum versus anisotropic factor for different values of refraction angle θ in YOZ plane.

6. SPECTRAL APPROACH OF IONOSPHERIC SCINTILLATION

R.m.s phase level and the scintillation level S_4 are computed as [19]:

$$< \varphi_1^2 >^{1/2} = \int_{-\infty}^{\infty} dk_x dk_y W_\varphi (k_x, k_y, z), \quad S_4^2 = \int_{-\infty}^{\infty} dk_x dk_y W_S (k_x, k_y, z), \tag{27}$$

where $W_S(k_x, k_y, z)$ is 2D scintillation spectrum (see below).

Scintillation of radio signals are related with the structure of ionospheric irregularities, i.e., with spatial-temporal behavior of electron density fluctuations. Irregularities of electron density embedded in the F-region impose an angular deviation of the incident radio wavefront that produces an interference pattern as the wave travels inside the turbulent collision magnetized plasma. The condition of a non-fully developed interference pattern is associated with significant Fresnel filtering factor; severe attenuation in the interference pattern of the long period fluctuations is associated with large irregularities. The standard relationship for weak scattering between the 2D scintillation spectrum and the 2D phase spectrum is given by [20]:

$$W_S\left(k_x, k_y, z\right) = 4W_\varphi\left(k_x, k_y, z\right)\sin^2\left(k_\perp^2/k_f^2\right), \tag{28}$$

where $k_\perp^2 = k_x^2 + k_y^2$, $k_f = (4\pi/\lambda z)^{1/2}$ is the Fresnel wavenumber. Scintillation level S_4 that gives additional information about the irregularities is expressed as follows [19]:

$$S_4^2 = \int\limits_{-\infty}^{\infty} dk_x dk_y W_S\left(k_x, k_y, z\right). \tag{29}$$

Equations (28) and (29) describe 2D diffraction pattern at the ground. Scintillation model is based on Gaussian irregularity. Substituting (17) into (28) and then into (29), after integration we obtain:

$$S_4^2 = 2 < \varphi_1^2 > G, \tag{30}$$

where

$$< \varphi_1^2 >= \sqrt{\pi}\sigma_N^2\left(D^2 + E^2\right)\frac{k_0^2\ell_\| z}{Q\chi}, \tag{31}$$

$$G = 1 - \left(1 + 4\frac{k_\perp^4}{k_f^4}\right)^{-1/4}\left(1 + 4\frac{k_\perp^2}{Q^4\chi^4 k_f^4}\right)^{-1/4} \cos\left(\frac{1}{2}arctg\frac{2k_\perp^2}{k_f^2} + \frac{1}{2}arctg\frac{2k_\perp^2}{Q^2\chi^2 k_f^2}\right)$$

is the Gaussian filtering factor. Equation (31) yields the relationship between the large-scale electron density irregularities and the emerging wavefront in terms of the phase spectrum. It is expressed through an anisotropy coefficient, angle of refraction of the wave and angle of inclination of prolate inhomogeneities with respect to the external magnetic field. The dependence of the level on the anisotropic features is illustrated in Figure 5 based on the Gaussian spectral form for different values of coefficient of anisotropy χ. The condition $k_\perp \ll k_f/\sqrt{2}$ is associate with a significant filtering, whereas $k_\perp \gg k_f/\sqrt{2}$ is associated with a fully developed diffraction pattern. The shaded area corresponds to a transition region between these two regions. Gaussian filtering factor $G \approx \left(k_\perp/\chi Q k_f\right)^4\left(1 + Q^2\chi^2\right)^2/2$ at $k_\perp \ll k_f/\sqrt{2}$ (or $\chi^2\lambda z \ll \ell_\|^2$) and is independent on χ at

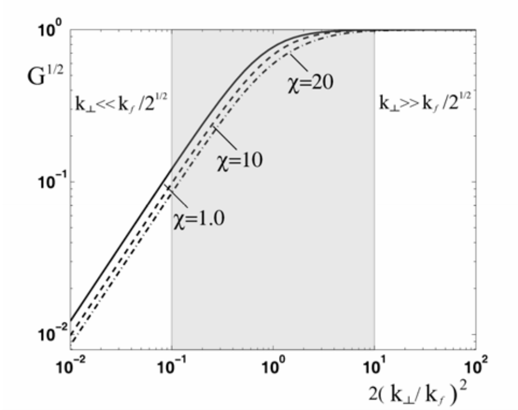

Figure 5. Scintillation level as a function of distance in the layer based on anisotropic Gaussian irregularities for different values of the anisotropic factor χ at $\theta = 0°$, $\alpha = 5°$.

$\chi Q \gg 1$, $G \approx 1$. For a fully developed interference pattern, Fresnel filtering is negligible [19]. Gaussian irregularities have been used for interpreting ionospheric scintillation measurements at meter wavelength. Numerical calculations have been carried out in F-region at a height 280 km for the basic frequency 40 MHz and under the following plasma parameters: $\sigma_N^2 = 10^{-6}$, $k_0\ell_\| = 5\cdot 10^3$, $z/\ell_\| = 100$. In this case $k_f = 1,67\,\text{km}^{-1}$, $k_\ell = 2\pi/\ell_\| = 1,05\,\text{km}^{-1}$. The interference pattern observing at the ground is an artifact of the Fresnel filtering attenuating factor and is associated with the left portion of Figure 5. The curves corresponding to different parameter of anisotropy are very close to each other, which demonstrate an internal consistency of the obtained results. Figure 6 illustrates the plots of variation of the normalized scintillation level S_4 as a function of $2\,(k_\perp/k_f)^2 = 2\chi^2\lambda z/\pi\ell_\|^2$ for anisotropic Gaussian power spectrum. It is clearly shown that at small distances the scintillation index S_4 increases and then, with increasing z, tends to saturation. Particularly, at $\chi = 10$, $\ell_\| = 6$ km, 40 MHz, starting with $z = 750$ km scintillation level tends to saturation. According to the experimental observations data S_4 is equal to 0.54 ± 0.04 at frequency 40 MHz [21]. From Figure 5 it could be easily shown that scintillation index reaches this value at distance $z = 98$ km from plasma-vacuum boundary at $\chi = 10$.

At $\sqrt{<\varphi_1^2>} < 1$ *radian* diffraction pattern on the ground such as correlation radius of the phase is equal to correlation radius of electron density fluctuation in the ionosphere [22]. In our case dispersion of

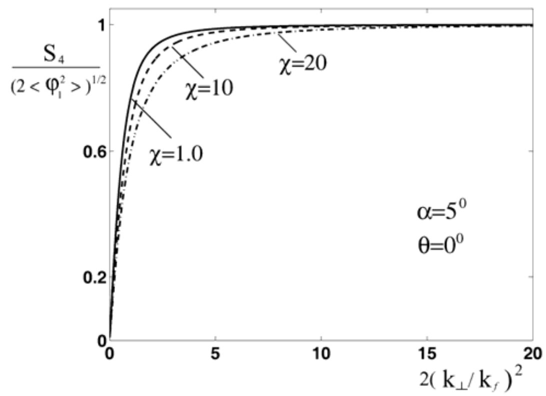

Figure 6. Normalized scintillation level as a function of distance in irregular layer based on anisotropic Gaussian irregularities for normal refraction of the wave $\theta = 0°$ and at angle of inclination of irregularities $\alpha = 5°$ for different values of the parameter of anisotropy χ.

Table 1.

θ (degree)	α (degree)	χ	$\sqrt{<\varphi_1^2>}$ (radian)	S_4 for $2\left(\frac{k_\perp}{k_f}\right)^2 = 10^{-1}$	S_4 for $2\left(\frac{k_\perp}{k_f}\right)^2 = 10$
10	5	1	0.4736	0.0802	0.6674
10	5	4	0.4610	0.0743	0.6493
10	5	20	0.3342	0.0399	0.4644
10	10	1	0.4736	0.0802	0.6674
10	10	4	0.4736	0.0802	0.6674
10	10	20	0.4736	0.0802	0.6674
30	5	1	0.5072	0.0769	0.7139
30	5	4	0.3662	0.0431	0.5069
30	5	20	0.1739	0.0194	0.2219
30	30	1	0.5072	0.0769	0.7139
30	30	4	0.5072	0.0769	0.7139
30	30	20	0.5072	0.0769	0.7139

the phase is equal to $\sqrt{<\varphi_1^2>} = 0.47$; 0.51 at $\theta = \alpha = 10°$; 30°, respectively. Moreover, variances of the phase and the scintillation levels for different θ, α and χ are summarized in Table 1. From the Table 1, it follows that an increase of parameter of anisotropy leads to decrease of variance of the phase at fixed ratio of θ: α. Numerical calculations show that S_4 is independent on parameter of anisotropy χ, when radio wave is propagating in turbulent magnetized plasma along the direction of prolate irregularities of electron density irregularities. Particularly, at $\theta = \alpha = 10°$, 30° index of scintillation is equal $S_4 \approx 0.08$ (the left portion of Figure 5) and $S_4 \approx 0.7$ (the right portion), respectively.

7. CONCLUSION

Statistical characteristics of the APS of scattered radiation have been investigated for both Gaussian and power-law spectra of electron density irregularities in the F-region of ionosphere. The applied theoretical formulation could be useful for developing a spectral model for F-region irregularities. The next step of our work is the investigation of an influence of magnetic field fluctuations on the APS in turbulent magnetized ionospheric plasma. Study of the spatial spectrum of multiply scattered radiation emitted by cylindrical antenna in a magneto-plasma [23, 24] is of a crucial importance under conditions of actual experiment.

REFERENCES

1. Ishimaru, A., *Wave Propagation and Scattering in Random Media*, Vol. 2, Multiple Scattering, Turbulence, Rough Surfaces and Remote Sensing, IEEE Press, Piscataway, New Jersey, USA, 1997.
2. Wernik, A. W., J. A. Secan, and E. J. Fremouw, "Ionospheric irregularities and scintillation," *Advances Space Research*, Vol. 31, No. 4, 971–981, 2003.
3. Xu, Z.-W., J. Wu, and Z.-S. Wu, "A survey of ionospheric effects on space-based radar," *Waves in Random Media*, Vol. 14, 189–273, 2004.
4. Gavrilenko, V. G., A. A. Semerikov, and G. V. Jandieri, "On the effect of absorption on multiple wave-scattering in magnetized turbulent plasma," *Waves in Random Media*, Vol. 9, 427–440, 1999.
5. Jandieri, G. V., V. G. Gavrilenko, A. V. Sorokin, and V. G. Jandieri, "Some properties of the angular power distribution

of electromagnetic waves multiply scattered in a collisional magnetized plasma," *Plasma Physics Report*, Vol. 31, No. 7, 604–615, 2005.

6. Jandieri, G. V., G. D. Aburjania, and V. G. Jandieri, "Transformation of the spectrum of scattered radiation in randomly inhomogeneous absorptive plasma layer," *Wave Propagation, Scattering and Emission in Complex Media*, Y.-Q. Jin (ed.), 207–214, Science Press, Beijing, China, World Scientific, Singapore City, Singapore, 2004.
7. Jandieri, G. V., V. G. Jandieri, Z. M. Diasamidze, I. N. Jabnidze, and I. G. Takidze, "Statistical characteristics of scattered microwaves in gyrotropic medium with random inhomogeneities," *International Journal of Microwave and Optical Technology*, Vol. 1, No. 2, 860–869, 2006.
8. Ginzburg, V. L., *Propagation of Electromagnetic Waves in Plasma*, Gordon and Beach, New York, 1961.
9. Eroglu, A. and J. K. Lee, "Dyadic Green's functions for an electrically gyrotropic medium," *Progress In Electromagnetics Research*, PIER 58, 223–240, 2006.
10. Eroglu, A. and J. K. Lee, "Wave propagation and dispersion characteristics for a nonreciprocal electrically gyrotropic medium," *Progress In Electromagnetics Research*, PIER 62, 237–260, 2006.
11. Rytov, S. M., Yu. A. Kravtsov, and V. I. Tatarskii, *Principles of Statistical Radiophysics*, Vol. 4, Waves Propagation through Random Media, Springer, Berlin, New York, 1989.
12. Cronyn, W. M., "The analysis of radio scattering and space-probe observations of small-scale structure in the interplanetary medium," *Astrophysics Journal*, Vol. 161, 755–763, 1970.
13. Chen, A. A. and G. S. Kent, "Determination of the orientation of ionospheric irregularities causing scintillation of signals from earth satellites," *Journal of Atmospheric and Terrestrial Physics*, Vol. 34, 1411–1414, 1972.
14. Shkarofsky, I. P., "Generalized turbulence space-correlation and wave-number spectrum-function pairs," *Canadian Journal of Physics*, Vol. 46, 2133–2153, 1968.
15. Abramowitz, M. and I. Stegun, *Handbook of Mathematical Functions*, Dover, 1972.
16. Gailit, T. A., V. D. Gusev, L. M. Erukhimov, and P. I. Shpiro, "On spectrum of phase fluctuations at ionospheric remote sensing," *Radiophysics*, Vol. 26, No. 7, 795–800, 1983 (in Russian).
17. Bakhmet'eva, N. V., V. N. Bubukina, Yu. A. Ignat'ev,

G. S. Bochkarev, V. A. Eremenko, V. V. Kol'sov, I. V. Krasheninnikov, and Yu. N. Cherkashin, "Investigation by backscatter radar irregularities produced in ionospheric plasma heating experiments," *Journal of Atmospheric and Terrestrial Physics*, Vol. 59, No. 18, 2257–2263, 1997.

18. Kravtsov, Yu. A., Yu. A. Feizulin, and A. G. Vinogradov, "Radio waves propagation through the Earth's atmosphere," *Radio and Communication*, Moscow, 1983 (in Russian).
19. Rufenach, C. L., "Ionospheric scintillation by a random phase screen: spectral approach," *Radio Science*, Vol. 10, No. 2, 155–165, 1975.
20. Bowhill, S. A., "Statistics of a radio wave diffracted by a random ionosphere," *J. Res. Nat. Bur. Stand., Sect. D*, Vol. 65D, 275–292, 1961.
21. Umeki, R., C. H. Liu, and K. C. Yeh, "Multifrequency spectra of ionospheric amplitude scintillation," *J. Geophysical Research*, Vol. 82, 2752–2760, 1977.
22. Kolosov, M. A., N. A. Armand, and O. I. Yakovlev, *Propagation of Radio Waves at Cosmic Communication*, Sviaz', Moscow, 1969 (in Russian).
23. Kudrin, A. V., E. Yu. Petrov, G. A. Kyriacou, and T. M. Zaboronkova, "Insulated cylindrical antenna in a cold magnetoplasma," *Progress In Electromagnetics Research*, PIER 53, 135–166, 2005.
24. Sten, J. C.-E. and A. Hujanen, "Aspects on the phase delay and phase velocity in the electromagnetic near-filed," *Progress In Electromagnetics Research*, PIER 56, 67–80, 2006.